Spin-Relaxation of Ho^{3+} in Yttrium Ethyl Sulfate between 1.2 and 25 K*†

M. D. Kemple‡ and H. J. Stapleton
Department of Physics and Materials Research Laboratory, University of Illinois, Urbana, Illinois 61801

(Received 10 September 1971)

T_1 was measured directly for samples containing 1 and 0.1 at.% Ho^{3+} using the method of pulse-saturation recovery between 1.1 and 3.5 K at *Ku*- and *X*-band frequencies. These data are interpreted as due to a sum of a phonon-limited direct relaxation process, a phonon-limited Orbach process which proceeds through an excited state with $\delta E/k = 8$ K, and a T^7 Raman process. Cross-relaxation effects among the hyperfine lines were noted in these T_1 data for the 1-at.% samples. Linewidths were also measured between 1.2 and 25 K and the more concentrated samples exhibited a minimum near 10 K. Above 15 K the relaxation-induced linewidth increased as T^7. The minimum in the linewidth is explained on the basis of decreased dipolar broadening, as the nonmagnetic state at 8 K is populated, followed by line broadening due to a dominant Raman relaxation mechanism. T_2/T_1 is estimated to lie between 0.9 and 1.8 for this T^7 Raman process.

I. INTRODUCTION

We have measured the spin-lattice relaxation rate of Ho^{3+} in yttrium ethyl sulfate [$Y(C_2H_5SO_4)_3 \cdot 9H_2O$ abbreviated YES] as a function of temperature using electron-paramagnetic-resonance techniques. Compared with most rare earths, YES: Ho possesses an extremely low-lying excited state $\delta E/k \simeq 8$ K, so that an Orbach relaxation mechanism contributes significantly even at temperatures as low as 1 K. The aim of this study was to determine if the Orbach relaxation mechanism was phonon limited, i.e., bottlenecked. Five earlier studies[1-5] over limited temperature regions did not conclusively answer this question. In this work, we have measured the spin-lattice relaxation time T_1 directly, using the method of pulse-saturation recovery (PSR) between 1.1 and 3.5 K at microwave frequencies near 9, 14, and 16 GHz. In addition we have measured the peak-to-peak widths ΔH of the derivatives of the absorption lines from 1.2 to 25 K. These measurements yielded the transverse relaxation time T_2 above 15 K, where the linewidth was relaxation broadened by a completely dominant Raman process. The observed linewidth of a sample containing 1 at.% Ho^{3+} was found to pass through a broad minimum near 10 K.

The general prediction for the temperature dependence of T_1 for a non-Kramers doublet is[6,7]

$$\frac{1}{T_1} = \begin{Bmatrix} A' \coth(h\nu/2kT) \\ D' \coth^2(h\nu/2kT) \end{Bmatrix} + \sum_i \frac{B_i}{e^{\delta E_i/kT} - 1} + CT^7 , \tag{1}$$

where T is the temperature of the thermal bath, δE_i is the energy of the ith excited state, and ν is the microwave frequency. The coth and $\coth^2$ terms represent either normal or phonon-limited direct processes. The terms in the summation correspond to Orbach relaxation mechanisms (either normal or phonon limited since the temperature dependence is unaltered) and the summation extends only over those states for which $\delta E_i/k$ is less than the Debye temperature Θ_D. An Orbach relaxation mechanism has been reported for samarium-doped lanthanum ethyl sulfate[8] with $\delta E/k$ equal to 72 K. The T^7 term in Eq. (1) represents the Raman process for a Debye model of the phonon spectrum and temperatures well below Θ_D.

If either the direct or Orbach relaxation processes are phonon limited, D' or B_i may be proportional to $\delta\nu/T_{ph}C$, where $\delta\nu$ is the frequency bandwidth of the interacting phonons, T_{ph} is their lifetime, and C is the concentration of the paramagnetic ions. Such a concentration dependence may be reduced in the direct process, if the phonon-limited relaxation rate is not appreciably slower than the normal direct-process rate. Under that condition the temperature dependence of the direct process is more complicated than shown in Eq. (1). Because the Orbach mechanism involves at least two different phonon energies centered about $\delta E \pm \frac{1}{2}h\nu$, overlap is possible and may reduce the concentration effects of a bottleneck in that relaxation process.[9,10]

II. EXPERIMENTAL DETAILS

The structure of YES and the rare-earth ethyl sulfates, in general, has been reviewed by Orbach.[6] The rare-earth site symmetry is C_{3h}. The spin Hamiltonian for YES: Ho has been given by Baker and Bleaney[11] as

$$\mathcal{H} = g_{\parallel}\mu_B H_z S_z + aI_z S_z + \Delta_x S_x + \Delta_y S_y , \tag{2}$$

with $S = \frac{1}{2}$, I(100% abundant Ho^{165}) $= \frac{7}{2}$, and the z axis is parallel to the threefold crystal symmetry axis. The last two terms reproduce the effects of random local distortions of the crystalline electrostatic field and in the absence of a hyperfine inter-

action give rise to a zero-field splitting of the doublet Δ equal to $(\Delta_x^2 + \Delta_y^2)^{1/2}$ which varies from one lattice site to another. The constants of the spin Hamiltonian are $g_{\parallel} = 15.36 \pm 0.04$, $a = 0.334 \pm 0.001$ cm^{-1}, and $\Delta_0 = 0.065 \pm 0.015$ cm^{-1}, where Δ_0^2 is the average value of Δ^2 over the distribution. All of our measurements were made with both the static and the microwave fields parallel to the crystal symmetry axis. The presence of the random strains allows resonance transitions to be induced between the electronic doublet under these experimental conditions. In addition microwave electric fields perpendicular to the crystalline axis are known to induce similar transitions.[12,13]

Single crystals of YES doped with small percentages of Ho^{3+} were grown slowly from saturated aqueous solutions by evaporation at 0 °C in a vacuum desiccator. YES was synthesized by a reliable method suggested to us by Mroczkowski.[14] Yttrium trichloride was made from 99.9999% rare-earth-purity yttrium oxide and reagent-grade hydrochloric acid. Yttrium trichloride was mixed with electronic-grade potassium ethyl sulfate in a water and ethyl alcohol solution from which potassium chloride precipitated leaving YES and the remainder of the potassium chloride in solution. The YES and potassium chloride were then separated in an absolute ethyl alcohol solution. Holmium ethyl sulfate with a rare-earth purity of 99.9% (available from A. D. Mackay, Inc.) was used as the doping agent by mixing together saturated solutions of HoEs and YES. The dopings in at.% refer to the relative volumes of these two saturated solutions from which the samples were grown. No attempt was made to determine the ratio of Ho^{3+} to Y^{3+} actually in the crystals. Typical samples were hexagonally shaped plates, 1 cm across and 0.5 cm thick.

Three different low-temperature microwave probes were employed; one for the *Ku*-band PSR measurements, one for the *Ku*-band linewidth measurements, and another for both types of measurements at *X* band. Carbon and germanium resistors were employed for temperature sensing. Details of the *Ku*-band spectrometer have been published.[15]

Superheterodyne detection was used for the PSR measurements and the relaxation times were extracted from the signal recoveries near thermal equilibrium since these recoveries were not singly exponential. These measurements were made by comparing the signal voltage against a known exponentially rising voltage on the *xy* axes of an oscilloscope. Relaxation times obtained in this manner had a typical accuracy of ±10% and were found to be independent of the saturating power (varied over a factor of 3), pulse duration (varied between factors of 20 and 100), and pulse rate frequency (varied between factors of 10 and 30). All reported relaxation times were determined with a pulse duration of 50 μsec.

For linewidth measurements, straight microwave-diode rectification was used, followed by narrow-band amplification and phase-sensitive detection at the 14-Hz magnetic field modulation frequency. Peak-to-peak derivative linewidths were measured along with line shapes on a strip-chart recorder as a function of temperature.

Data were computer fitted to various theoretical temperature dependences using a least-squares fitting routine which allowed for nonlinear parameters.

III. RESULTS

A. Linewidth Data

Measurements were made on three crystals, two with a nominal Ho^{3+} doping of 1 at.% (samples *A* and *B*), and one with a doping of 0.1 at.% (sample *C*). Linewidth and PSR data were taken on sample *A* at *Ku*- and *X*-band microwave frequencies and for sample *C* at *Ku* band. Only *Ku*-band PSR measurements were made on sample *B*. Of the eight hyperfine lines, only the three highest-field lines ($I_z = -\frac{7}{2}$, $-\frac{5}{2}$, and $-\frac{3}{2}$) were extensively studied since the magnetic field positions of these transi-

TABLE I. Variation of the observed peak-to-peak derivative linewidth with temperature for sample *A* (1 at.% Ho) and *C* (0.1 at.% Ho) at various frequencies.

	Sample *A* 17.49 GHz	Sample *A* 8.82 GHz $I_z = -\frac{7}{2}$	Sample *C* 16.22 GHz
T (K)	ΔH (Oe)	ΔH (Oe)	ΔH (Oe)
1.2	13.3 ± 0.4		7.5 ± 0.1
1.50		13.7 ± 0.3	
2.50	12.7 ± 0.4		
2.80		13.5 ± 0.2	
4.22	14.1 ± 0.4	12.7 ± 0.2	7.2 ± 0.2
7.00	12.8 ± 0.4	12.2 ± 0.1	7.1 ± 0.3
9.00	11.9 ± 0.4		
10.0	11.6 ± 0.4	12.0 ± 0.3	7.4 ± 0.3
11.0	11.4 ± 0.4	12.0 ± 0.2	
12.0	12.1 ± 0.5	12.2 ± 0.3	7.7 ± 0.5
13.0	12.0 ± 0.4		
14.0		13.2 ± 0.3	
14.5	13.0 ± 0.4		
15.0			11.7 ± 1.2
16.0	15.4 ± 0.5	16.1 ± 0.5	
17.5	19.6 ± 0.6		
18.0		21.1 ± 0.6	
19.0	26.2 ± 1.3	25.7 ± 0.6	
20.0		30.5 ± 2.2	
20.5	36.4 ± 3.7		
22.0	55.9 ± 3.7	44.5 ± 1.5	
23.0		57.3 ± 2.7	
25.0		75.2 ± 3.3	

tions were well separated from the others. The eight positions calculated from Eq. (2) at 16.35 GHz are 2382, 1918, 1453, 989, 869, 524, 405, and 59.8 Oe.

We consider first the linewidth measurements which are given in Table I. No designation is made with respect to I_z at *Ku*-band frequencies since the three lines, all symmetric, give the same peak-to-peak derivative width within experimental error. At *X* band, only data for the highest-field line ($I_z = -\frac{7}{2}$) are tabulated since the $I_z = -\frac{5}{2}$ and $-\frac{3}{2}$ lines were asymmetric and had different widths. It is interesting to note that sample *A* (1 at.% Ho^{3+}) clearly shows a minimum width near 10 K. A similar effect for sample *C* (0.1 at.% Ho^{3+}) is only marginally observable, at best. One plausible explanation of this phenomenon depends critically upon the nature of the dominant relaxation process at these higher temperatures, so further discussion will be postponed.

The observed peak-to-peak derivative linewidth ΔH must be corrected for that component ΔH_0 which is not connected with relaxation mechanisms. The method by which the relaxation-induced peak-to-peak derivative linewidth $\Delta H'$ is extracted from ΔH and ΔH_0 depends upon the line shapes associated with each broadening mechanism. The relaxation-induced line shape is Lorentzian while the low-temperature line shape is generally approximated as either Lorentzian or Gaussian. For a Lorentzian-Lorentzian convolution

$$\Delta H' = \Delta H - \Delta H_0 \ , \tag{3}$$

and for a Lorentzian-Gaussian convolution

$$\Delta H' \approx F(\Delta H, \Delta H_0) \ , \tag{4}$$

where $F(\Delta H, \Delta H_0)$ is an analytic function, formulated by Stoneham,[16] which approximates the effects of such a convolution to better than 1% accuracy for all ratios of $\Delta H'/\Delta H_0$.

The transverse relaxation time T_2 is defined in terms of the full width $\Delta\omega_{1/2}$ (in rad/sec) at half-amplitude of a Lorentzian-shaped relaxation-broadened absorption line as follows:

$$\frac{1}{T_2} = \tfrac{1}{2}\Delta\omega_{1/2} = \frac{g\mu_B \Delta H_{1/2}}{2\hbar} = \sqrt{3}\,\frac{g\mu_B \Delta H'}{2\hbar}$$

$$= (7.62\times 10^6) g \Delta H' \ , \tag{5}$$

where g is the spectroscopic splitting factor of the transition.

Two complications arise in determining $\Delta H'$ from the data of sample *A* in Table I. First, the low-temperature linewidths exhibited a broad minimum and second, the line shape at this minimum is midway between Gaussian and Lorentzian. We have taken ΔH_0 to be the minimum linewidth and have treated the data in two ways, using either Eq. (3) or (4) appropriate to Lorentzian-Lorentzian or Lorentzian-Gaussian convolutions, respectively. Values of $1/T_2$ were subsequently obtained through the use of Eq. (5) with $g = g_{\parallel} = 15.4$ and the *Ku*-band results are shown in Fig. 1. Curves representing fits to a T^7 dependence are also shown. The three lowest-temperature points have a large uncertainty because of the small value of $\Delta H'/\Delta H_0$, and fall slightly below the fitting curves. If these three points are omitted and separate fits are made of these data to a T^n power law, the optimum value of n is 7.1 ± 0.4. Similar fits of the *X*-band linewidth data for sample *A* (not shown) produced optimum n values between 5 and 7 depending upon the convolution and the number of points fitted. Fits were also attempted for these data in which an Orbach process with $\delta E/k$ values of 8 or 66.8 K (the second excited state) was included, but the results were inconsistent between the two convolutions used and also with the PSR data taken at lower temperatures. The values of $1/T_2$ fit well to an exponential temperature dependence of the form $e^{-130/T}$ but this exceeds estimated values of Θ_D for rare-earth ethyl sulfates[17] by nearly a factor of 2

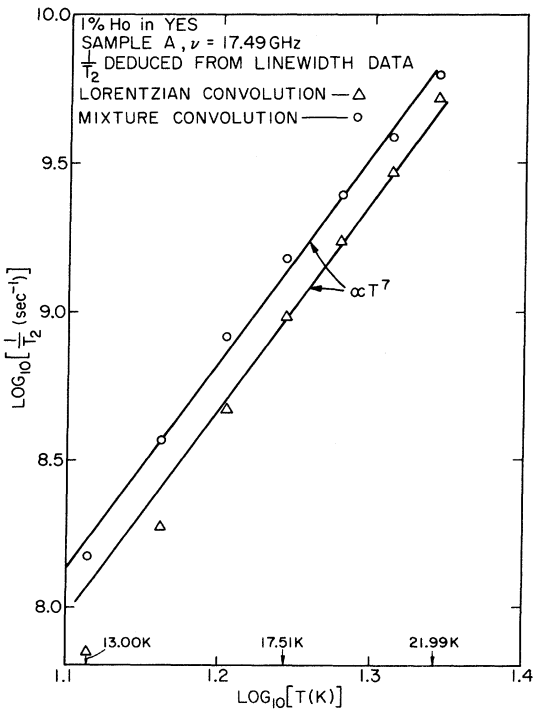

FIG. 1. Temperature dependence of the transverse relaxation rate, $1/T_2$, of the $I_z = -\frac{3}{2}$, $-\frac{5}{2}$, and $-\frac{7}{2}$ hyperfine lines of sample *A* (1 at.% Ho in YES) at 17.49 GHz. The rates were deduced from the linewidth data by considering two different convolutions, Lorentzian-Lorentzian and Gaussian-Lorentzian (mixture), of the lifetime and nonlifetime components of the resonance lines as explained in the text.

and furthermore does not correspond to any energy level of YES: Ho.[18] Such a temperature dependence could represent relaxation via optical phonons.[19] However the presence of a T^7 process is consistent with our PSR data to be discussed later and also with the work of others on rare-earth ethyl sulfates.[7,8] In all further analysis we assume these data to be described by a T^7 process.

The linewidth data on sample C were too meager to be of value in determining T_2, but the absence of a clearly defined minimum will be of interest in later discussion.

B. PSR Data

PSR measurements of $1/T_1$ were made between 1.1 and 3.5 K. Figure 2 shows the Ku-band data on samples A and C. The curve in Fig. 2 indicates the temperature dependence associated with an Orbach process with $\delta E/k = 8$ K. It can be seen that the relaxation is dominated by this Orbach process over a significant portion of the temperature range. Note also that the relaxation rates of the three hyperfine lines were different for sample A, while for sample C (0.1 at.% Ho^{3+}) there were no observable differences among the hyperfine lines.

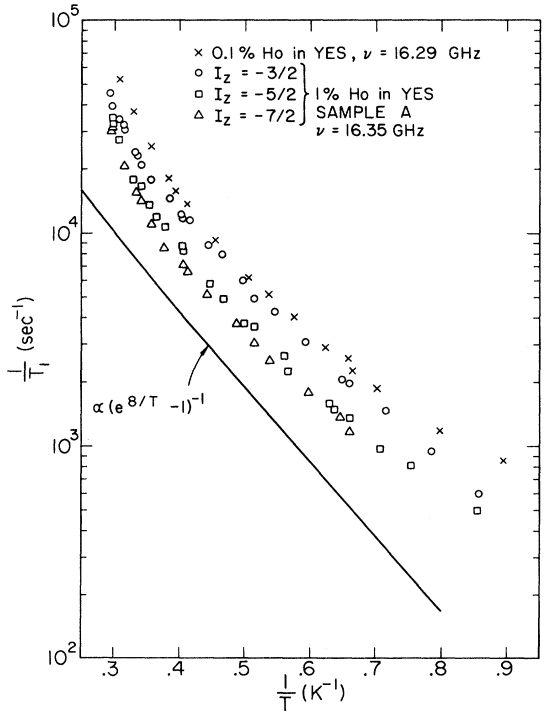

FIG. 2. Temperature dependence of the relaxation rates of the $I_z = -\frac{3}{2}$, $-\frac{5}{2}$, and $-\frac{7}{2}$ hyperfine lines of sample A (1 at.% Ho in YES) and sample C (0.1 at.% Ho in YES) as deduced from PSR data at Ku-band frequencies. For sample C the relaxation rates of these three hyperfine lines were the same within a maximum spread of ±7% and the averages are plotted.

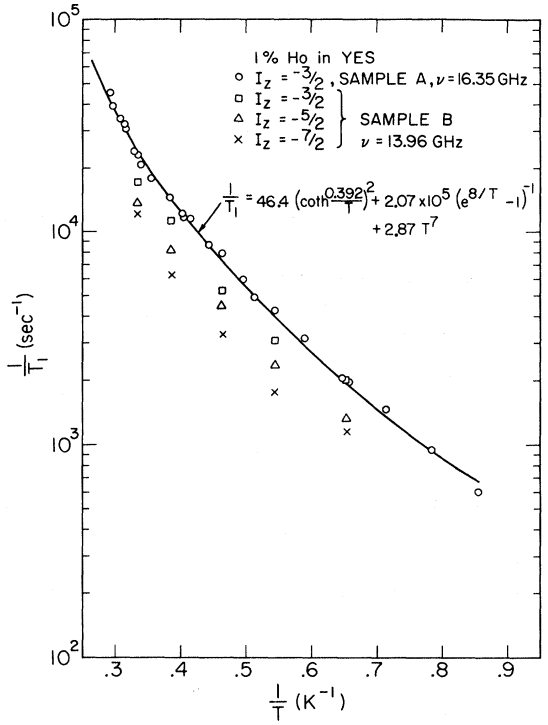

FIG. 3. Temperature dependence of the relaxation rate of the $I_z = -\frac{3}{2}$ hyperfine line of sample A (1 at.% Ho in YES) at 16.35 GHz. Also shown is the temperature dependence of $1/T_1$ for the $I_z = -\frac{3}{2}$, $-\frac{5}{2}$, and $-\frac{7}{2}$ hyperfine lines of sample B (also 1 at.% Ho) at 13.96 GHz.

Figures 3–5 show additional PSR data on the two samples containing 1 at.% Ho^{3+}. We note from these figures that the relaxation rates of these two samples differ by 20–30%. Computer fits of the Ku-band data for sample A are also indicated in these figures. In Sec. III C, we discuss the details of these fits.

C. Fitting Temperature Dependence of Data

The Ku-band T_1 and T_2 data for sample A and the Ku-band T_1 data of sample C were fitted to Eq. (1). Since for sample A, the T_2 and T_1 data were taken at 17.49 and 16.35 GHz, respectively, a common fit of these two sets of data involves the implicit, but reasonable assumption, that the T^7 relaxation process, which completely dominates the T_2 data, is independent of frequency. The frequency which appears explicitly in the direct process was, of course, set equal to the value used in the T_1 measurements. Some ambiguity exists as to the appropriate value of δE to be used in the Orbach process involving the first excited state. Optical measurements by Grohmann *et al.*[18] suggest $\delta E/k$ changes from 6.96 to 8.65 K as the temperature drops from 58 to 4.2 K. Baker and Bleaney[20] arrived at a δE value between 5.5 and 5.6 cm^{-1}. We chose $\delta E/k$

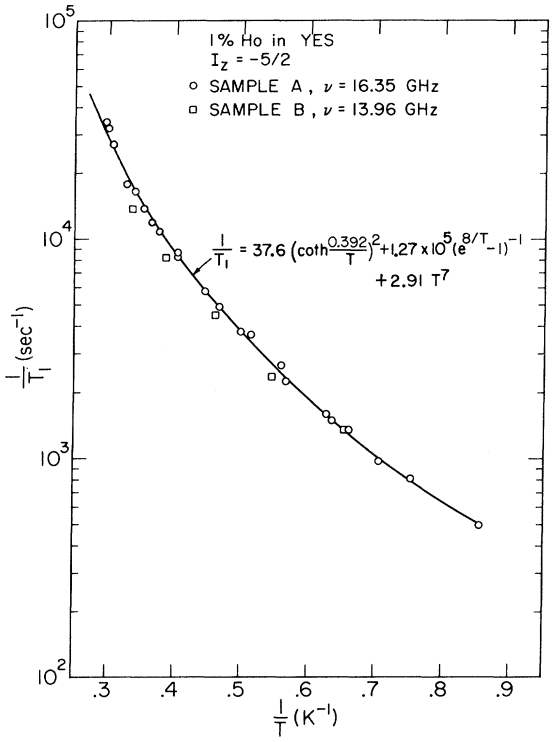

FIG. 4. Temperature dependence of the relaxation rate of the $I_z = -\frac{5}{2}$ hyperfine line of two 1-at.% YES: Ho samples, A and B, at 16.35 and 13.96 GHz, respectively.

$= 8\,\mathrm{K}$ ($\delta E = 5.55\ \mathrm{cm}^{-1}$) for our fits. This value fell in the midrange of those giving the best fits.

In order to fit the T_1 data with the T_2 data we must know the ratio T_2/T_1. Various authors have recently discussed this problem for the situation where T_2 is dominated by the phonon-induced lifetime and find that T_2/T_1 depends upon the specific relaxation mechanism. The Orbach process has been treated by Culvahouse and Richards[21] and the Raman process has been considered by Stedman.[22] Since the T_2 data are dominated by a T^7 Raman process, we consider only that case. Stedman finds that the full frequency width at half-maximum of the resonance absorption line, $2/T_2$, is composed of two parts. One is related to the thermal equilibration of the level populations and is just $1/T_1$. The other contribution involves self-energy processes, which do not change the level populations, but shorten the phase memory time T_2. It is difficult to evaluate the strength of this contribution, Γ, but the general prediction which can be made for Raman processes is that

$$2/T_2 = 1/T_1 + \Gamma \tag{6}$$

or

$$T_2/T_1 \leq 2\ . \tag{7}$$

Since we had no definite prediction for this self-energy term, we elected to determine T_2/T_1 from our experimental data on sample A. To do this in a consistent manner, we first fit the T_1 data for each of the three hyperfine lines to Eq. (1) assuming a bottlenecked direct process, since this gave consistently better fits than the use of a normal direct process. We then fit the linewidth data to a T^7 power law using both types of line-shape convolutions and compared these results with the coefficient of T^7 in the PSR data. The results were

$$T_2/T_1 = 1.06 \pm 0.19$$

(Lorentzian-Gaussian convolution) (8a)

or

$$T_2/T_1 = 1.52 \pm 0.27$$

(Lorentzian-Lorentzian convolution). (8b)

Since the actual line shape at minimum linewidth was midway between Gaussian and Lorentzian, presumably the true T_2/T_1 ratio lies between these values so we conclude

$$0.9 \leq T_2/T_1 \leq 1.8 \tag{8c}$$

for a T^7 Raman process.

Using the T_2/T_1 factor [(8a) or (8b)] appropriate to the convolution, a fit of both linewidth and PSR data was made for each of the three hyperfine lines. The resulting fits were essentially independent of the convolution employed, and the strength of the

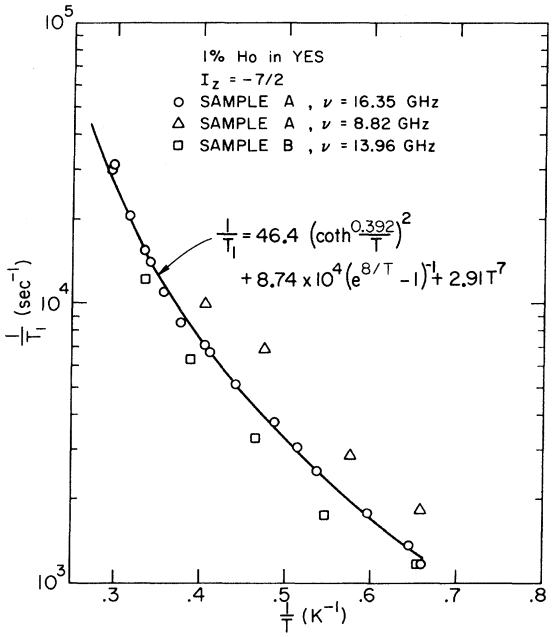

FIG. 5. Temperature dependence of the relaxation rate of the $I_z = -\frac{7}{2}$ hyperfine line of two 1-at.% YES: Ho samples, A and B, at various microwave frequencies.

Raman process was about the same for each line because it is primarily determined by the linewidth data. Figure 6 shows such a complete fit for one of the hyperfine lines of sample A. In the case of sample C (0.1 at.% Ho^{3+}) only the PSR data taken at 16.29 GHz were fit to Eq. (1). Table II indicates various fits of the data from sample C along with the fits of the hyperfine data of sample A. No differences were observed among the hyperfine states of sample C so no I_z designation has been made.

The results of these computer fits are consistent with the existence of a phonon bottleneck in both the direct and Orbach relaxation mechanisms. In particular the relaxation is faster for the 0.1-at.% sample than for either of the 1-at.% samples. The $\Delta\nu/C$ dependence is not as strong as predicted by the simplest models, but recent measurements on Ce^{3+} and Nd^{3+} in lanthanum magnesium nitrate[23,24] nave given definite indications of a phonon-limited Orbach process with a concentration dependence which is weaker than $\Delta\nu/C$. It is also possible in the case of YES: Ho that cross relaxation among the paramagnetic ions contributes to the weaker concentration dependence. Further comments on this will be given in Sec. IV.

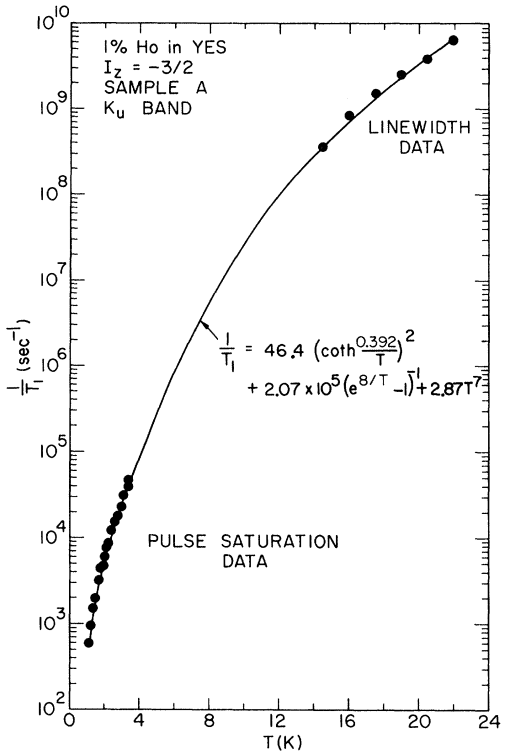

FIG. 6. Temperature dependence from 1.1 to 22 K of the relaxation rate of the $I_z = -\frac{3}{2}$ hyperfine line of 1 at.% Ho in YES (sample A) measured at Ku-band frequencies. For points in the upper temperature region, $1/T_1$ was determined from $1/T_2$ measurements.

IV. FURTHER DISCUSSION

A. Linewidth Minimum

We can give a plausible explanation for the linewidth minimum observed for sample A at Ku- and X-band frequencies. It is based on magnetic dipole interactions between the paramagnetic ions and the non-negligible population of the excited singlet at 8 K when temperatures are of the order of 10 K. As more and more ions are excited into this nonmagnetic state, the dipolar linewidth should decrease. Noting that for Ho^{3+} concentrations under a few percent the dipolar broadening should be directly proportional to the concentration, and applying Boltzmann statistics, we can write the dipolar contribution to the linewidth as

$$\Delta H_{\rm dip} = 2G/(2+e^{-8/T}) \quad , \tag{9}$$

where we have neglected the separation of the ground-state doublet with respect to kT. G, which represents the dipolar width for $T \ll 8$ K, is independent of T when $h\nu \ll kT$. We can estimate G by comparison of our linewidth data for samples A and C, and also by applying a formula given by Mims *et al.*[25] For a 1% sample, the two methods yield 6 and 12 Oe, respectively, in terms of the peak-to-peak derivative linewidth. These estimates, inserted into Eq. (9), yield a decrease in the linewidth with temperature on the order of that observed

TABLE II. Resulting parameters from fits of the data to Eq. (1) with $h\nu/2k = 0.392$ K. The numbers in the column labeled VAR are proportional to the weighted variance of each fit.

Sample	Ho (at.%)	I_z	A' (sec^{-1})	D' (sec^{-1})	B (sec^{-1})	C (sec^{-1} K^{-7})	VAR
A	1	$-\frac{3}{2}$		46.4	2.07×10^5	2.87	2.6
A	1	$-\frac{5}{2}$		37.6	1.27×10^5	2.91	2.2
A	1	$-\frac{7}{2}$		46.4	8.74×10^4	2.91	2.6
C[a]	0.1			81.4	1.77×10^5	7.46	1.0
C[a]	0.1		200		2.95×10^5	2.90[b]	4.9
C[a]	0.1			66.0	2.57×10^5	2.90[b]	5.7

[a]PSR data only. No differences were observed among the three hyperfine lines studied at this lower concentration.
[b]Parameter held fixed.

for sample A and are consistent with the fact that the linewidth minimum was not resolvable for the 0.1% sample. If a T^7 temperature dependence, representing lifetime broadening, is added to Eq. (9) then the resultant function possesses a minimum. In particular for the estimates of G and the observed strength of the T^7 line broadening on sample A, this linewidth minimum occurs in the temperature range between 8 and 10 K, in reasonable agreement with observations.

If an Orbach relaxation mechanism is added to Eq. (9) so that

$$\Delta H = \frac{2G}{2+e^{-\delta/T}} + \frac{B}{e^{\delta/T}-1} \quad , \tag{10}$$

then no linewidth minimum is possible if B exceeds $\frac{1}{2}G$. Clearly if the observed linewidth were dominated by an Orbach process of this type, B would exceed $\frac{1}{2}G$ and no minimum should be observed. Therefore the existence of a linewidth minimum is additional evidence that the Orbach relaxation process, observed in the pulse-saturation data, is negligible at temperatures where the lines broaden.

We now comment briefly on the line shapes below 14 K. At the Ku band all eight hyperfine lines of sample A were symmetric, while at the X band one line was very asymmetric (signal amplitudes at the two derivative peaks differing by a factor of 2), four were moderately asymmetric, and three others were symmetric. None of the low-temperature linewidths of sample A were equal at the X band. As the temperature was raised above 14 K the very asymmetric line became symmetric and Lorentzian as lifetime broadening dominated. The existence of symmetric resonance lines at low temperatures is surprising for this non-Kramers ion. The random strains discussed earlier are expected to produce asymmetric line shapes.[20]

Figures 2 and 3 indicated that T_1 had a hyperfine dependence in the temperature range 1.1–3.5 K at concentrations of 1 at.%, but no such dependence at one-tenth that concentration. Furthermore, the $I_z = -\frac{3}{2}$ transition relaxed faster than the $I_z = -\frac{5}{2}$ transition, which in turn relaxed faster than the $I_z = -\frac{7}{2}$ transition. This would suggest cross-relaxation mechanisms involving $l:m:n$ multiple spin flips among ions in different hyperfine states. For example, energy is approximately conserved if two ions in an $I_z = -\frac{3}{2}$ state make a downward spin flip while one ion each in the $I_z = -\frac{1}{2}$ and $-\frac{5}{2}$ states makes upward spin flips. Such a mechanism would be concentration dependent and qualitatively show the I_z dependence observed.

It is also worth noting that the I_z dependence in Figs. 2 and 3 does not depend upon the temperature, or more precisely, the dominant relaxation mechanism, but rather each curve of data points is displaced almost uniformly. This would appear to rule out the influence of wave-function admixtures due to a hyperfine interaction proportional to $\vec{I} \cdot \vec{J}$.[26,27] The fact that this I_z effect is independent of frequency and dependent upon concentration argues against it being associated with impurities.

B. Conclusion

We conclude from these data that the direct and Orbach relaxation rates are phonon limited for the concentrations studied, and that the low-temperature relaxation rates were affected by cross-relaxation processes. Furthermore, at temperatures above 15 K, we find the relaxation mechanism to be described by a T^7 Raman process which completely dominates any Orbach mechanism involving the excited state with $\delta E/k$ equal to 8 K. In addition a minimum in the linewidth was found for a sample containing 1 at.% Ho and this is consistent with a model involving dipolar broadening, an excited singlet at 8 K, and a dominant Raman relaxation process. The fitting of the data was by no means unique, but we consider the fits reported here to be the most reasonable ones, compatible with both the linewidth and PSR data.

---

*Work supported in part by the Advanced Research Projects Agency under Contract No. HC 15-67-C-0221.

†Paper based upon a dissertation submitted by M. D. Kemple in partial fulfillment of the requirements for the Ph.D. degree at the University of Illinois.

‡Present address: Enrico Fermi Institute and the Department of Chemistry, The University of Chicago, Chicago, Ill.

[1]L. J. Raubenheimer, Ph.D. thesis (University of Illinois, 1964) (unpublished).

[2]Heinz Kalbfleisch, Z. Physik 181, 13 (1964).

[3]S. Hüfner and G. Weber, Phys. Letters 13, 115 (1964).

[4]R. Cremer, N. Gabrielsen, S. Hüfner, G. Nicolay, and G. Weber, Physik Kondensierten Materie 5, 5 (1966).

[5]A. H. Cooke and E. J. Daintree, in *Proceedings of the Third Conference on Rare Earth Research* (Gordon and Breach, New York, 1964), p. 401.

[6]R. Orbach, Proc. Roy. Soc. (London) A264, 458 (1961).

[7]P. L. Scott and C. D. Jeffries, Phys. Rev. 127, 32 (1962).

[8]G. H. Larson and C. D. Jeffries, Phys. Rev. 141, 461 (1966).

[9]W. J. Brya and P. E. Wagner, Phys. Rev. 147, 239 (1966).

[10]R. C. Sapp, Bull. Am. Phys. Soc. 16, 360 (1971).

[11]J. M. Baker and B. Bleaney, Proc. Phys. Soc. (London) A68, 1090 (1955).

[12]F. I. B. Williams, Proc. Phys. Soc. (London) 91, 111 (1967).

[13]J. W. Culvahouse, David P. Schinke, and Donald L. Foster, Phys. Rev. Letters 18, 117 (1967).

[14]S. Mroczkowski (private communication).

[15]Thomas L. Bohan and H. J. Stapleton, Rev. Sci.

Instr. 39, 1707 (1968).
[16]A. M. Stoneham (private communication).
[17]J. C. Gill, Proc. Phys. Soc. (London) 82, 1066 (1963).
[18]I. Grohmann, K. H. Hellwege, and H. G. Kahle, Z. Physik 164, 243 (1961).
[19]Chao-Yuan Huang, Phys. Rev. 154, 215 (1967).
[20]J. M. Baker and B. Bleaney, Proc. Roy. Soc. (London) A245, 156 (1958).
[21]J. W. Culvahouse and Peter M. Richards, Phys. Rev. 178, 485 (1969).
[22]G. E. Stedman, J. Phys. C 3, 2392 (1970).
[23]Gh. Cristea and H. J. Stapleton, in *Proceedings of the Sixteenth Colloque Ampère* (North-Holland, Amsterdam, to be published).
[24]Gh. Cristea, T. L. Bohan, and H. J. Stapleton, Phys. Rev. B 4, 2081 (1971).
[25]W. B. Mims, K. Nassau, and J. D. McGee, Phys. Rev. 123, 2059 (1961).
[26]J. M. Baker and N. C. Ford, Jr., Phys. Rev. 136, A1692 (1964).
[27]G. H. Larson and C. D. Jeffries, Phys. Rev. 145, 311 (1966).

PHYSICAL REVIEW B VOLUME 5, NUMBER 5 1 MARCH 1972

Microwave Dielectric Loss of V^{+4}-Doped TiO_2 at Low Temperatures*

L. G. Rowan
Physics Department, University of North Carolina, Chapel Hill, North Carolina 27514
(Received 9 August 1971)

The dielectric loss of rutile doped with 0.05% vanadium impurities is measured at low temperatures and at 10 GHz. The electron-hopping frequency $1/\tau$ has a temperature dependence given by $(1.5\times 10^{10})e^{-220/T}$. The model of Dominik and MacCrone of a hopping electron between the V^{+4} ion and the Ti^{+3} ion is consistent with the data. The motion of the electron from the vanadium site is observed by electron–spin-echo techniques.

I. INTRODUCTION

The dielectric properties of rutile have been studied by many investigators.[1] The various types of defects that can occur in rutile have been discussed by Von Hippel *et al.*[2] The dielectric relaxation in rutile at low temperatures has been studied by Dominik and MacCrone.[3] In their work, they present data that can be explained by the model of an electron hopping between titanium lattice sites. We present in this paper further data on dielectric loss at low temperatures and at microwave frequencies that can also be explained by the hopping-electron model.

We have measured the dielectric loss of nominally pure rutile and rutile doped with vanadium impurities over the temperature range of 1.6 to 30 °K. We will discuss our experimental procedures and results, and then use the hopping-electron model to explain the experimental results. We will mention some electron-paramagnetic-resonance results that support this model.

II. EXPERIMENTAL PROCEDURE

A procedure for measuring the dielectric constant and loss tangent of rutile at microwave frequencies and low temperatures has been discussed by Sabisky and Gerritsen.[4] Since the dielectric constant of rutile is so high (~100), a sample of about 0.5 cm^3 in volume can have dielectric modes[5] at X-band frequencies which can be easily coupled to the waveguide modes.

For a microwave cavity, the decay time t_d is given by

$$t_d = Q/\pi f ,$$

where Q is the quality factor of the cavity and f is the microwave resonant frequency. The Q factor is defined as the maximum stored energy divided by the average energy loss per radian. For a cavity in which all the energy is dissipated in a low-loss dielectric, the Q factor is given by

$$Q = \epsilon_1/\epsilon_2 = 1/\tan\delta ,$$

where ϵ_1 is the real part of the dielectric constant, ϵ_2 is the imaginary part, and $\tan\delta$ is the loss tangent. Thus we see that

$$1/t_d = \pi f \tan\delta .$$

Our procedure for measuring the loss tangent is to excite one of the dielectric modes of the rutile crystal with a very short microwave pulse. Then we observe the exponential decay of the dielectric modes after the excitation and record the decay rate $1/t_d$. The dielectric modes are very similar to the TM modes of a circular cylinder. For a TM_{01} mode there are electric fields in both the axial direction and the radial direction of the circular cavity. However, for rutile with its high dielectric constant, the electric field in the axial direction is more than ten times larger than the radial electric field. Therefore, we will assume